Two-Dimensional Reaction Free Energy Surfaces of Catalytic Reaction: Effects of Protein Conformational Dynamics on Enzyme Catalysis†

Wei Min, X. Sunney Xie,* and Biman Bagchi*,‡

Department of Chemistry and Chemical Biology, Harvard University, Cambridge, Massachusetts 02138

Received: August 14, 2007; In Final Form: October 23, 2007

We introduce a two-dimensional (2D) multisurface reaction free energy description of the catalytic cycle that explicitly connects the recently observed multi-time-scale conformational dynamics as well as dispersed enzymatic kinetics to the classical Michaelis−Menten equation. A slow conformational motion on a collective enzyme coordinate *Q* facilitates the catalytic reaction along the intrinsic reaction coordinate *X*, providing a dynamic realization of Pauling's well-known idea of transition-state stabilization. The catalytic cycle is modeled as transitions between multiple displaced harmonic wells in the *XQ* space representing different states of the cycle, which is constructed according to the free energy driving force of the cycle. Subsequent to substrate association with the enzyme, the enzyme−substrate complex under strain exhibits a nonequilibrium relaxation toward a new conformation that lowers the activation energy of the reaction, as first proposed by Haldane. The chemical reaction in *X* is thus enslaved to the down hill slow motion on the *Q* surface. One consequence of the present theory is that, in spite of the existence of dispersive kinetics, the Michaelis−Menten expression of the catalysis rate remains valid under certain conditions, as observed in recent single-molecule experiments. This dynamic theory builds the relationship between the protein conformational dynamics and the enzymatic reaction kinetics and offers a unified description of enzyme fluctuation-assisted catalysis.

1. Introduction

How enzymes catalyze biochemical reactions has remained one of the oldest and most challenging problems in chemistry. Without the enzyme, the same biochemical reaction would still take place in aqueous solution, but at a vastly slower rate, with half times ranging from hours all the way up to a billion years.[1] The typical enzymatic acceleration lies in the region of 10^8−10^{12},[1] involving molecular recognition at the highest level of evolutionary development.

A general approach to study enzyme catalysis is to probe the dependence of catalytic velocity on the substrate concentration [S]. The celebrated Michaelis−Menten (MM) equation[2] satisfactorily describes the kinetics of many enzymes with the following picture: A substrate molecule S physically diffuses close to an enzyme E and binds reversibly to it, forming an enzyme−substrate complex ES that then undergoes unimolecular catalytic conversion to an enzyme−product complex EP, which could further undergo product release, regenerate the original enzyme E, and resume a new cycle:

$$\mathrm{S} + \mathrm{E} \underset{k_{-1}}{\overset{k_1^0}{\rightleftharpoons}} \mathrm{ES} \underset{k_{-2}}{\overset{k_2}{\rightleftharpoons}} \mathrm{EP} \underset{k_{-3}^0}{\overset{k_3}{\rightleftharpoons}} \mathrm{E} + \mathrm{P}$$

Note that the diffusion of substrate and product molecules toward the enzyme have been implicitly included in the pseudo first-order binding constants k_1^0 and k_{-3}^0, respectively. When the product release step is fast and the concentration of product is negligible, one has the following simpler form:

$$\mathrm{S} + \mathrm{E} \underset{k_{-1}}{\overset{k_1^0}{\rightleftharpoons}} \mathrm{ES} \xrightarrow{k_2} \mathrm{E} + \mathrm{P}$$

Under the steady-state (i.e., the concentration of ES no longer depends on time) condition, the rate of enzyme-catalyzed product formation v has a hyperbolic dependence on [S]:

$$v = \frac{k_2[\mathrm{S}]}{[\mathrm{S}] + K_\mathrm{M}} \tag{1.1}$$

where the Michaelis constant $K_\mathrm{M} \equiv (k_{-1} + k_2)/k_1^0$.

Figure 1 illustrates the reaction free energy surface of the enzyme-catalyzed reaction, as is shown in many biochemistry textbooks. The horizontal axis is often referred to as the "reaction progress", which is somewhat ill-defined because the first step, E + S → ES, is a bimolecular reaction. ES → EP is a unimolecular reaction, for which an intrinsic reaction coordinate (IRC) of the chemical reaction can be defined. Lowering the free energy activation barrier for the ES → EP step compared to that of the uncatalyzed reaction S → P is the most significant effect of the enzyme−substrate complex responsible for the dramatic increase of reaction rate, which is referred to as "transition-state stabilization" by Pauling.

However, the enzyme and enzyme−substrate complex are dynamic entities. It is now generally believed that the flexibility and dynamics of proteins play an important role in enzymatic function.[3−6] However, the detailed relationship between conformational fluctuation and chemical kinetics is still not well understood at the theoretical level, partly because of the broad range of time scales of enzyme conformational dynamics, ranging from a few tens of femtoseconds to 100 s. The fast conformational dynamics on the time scale of femtoseconds to microseconds can be probed by molecule dynamics simulations.[5,7] However, most enzymatic reactions occur at much

† Part of the "James T. (Casey) Hynes Festschrift".

* Authors to whom correspondence should be addressed. Electronic mail: xie@chemistry.harvard.edu (X.S.X.); bbagchi@sscu.iisc.ernet.in (B.B.).

‡ Permanent address: Solid State and Structural Chemistry Unit, Indian Institute of Science, Bangalore 560012, India.

10.1021/jp076533c CCC: $40.75
Published on Web 12/18/2007

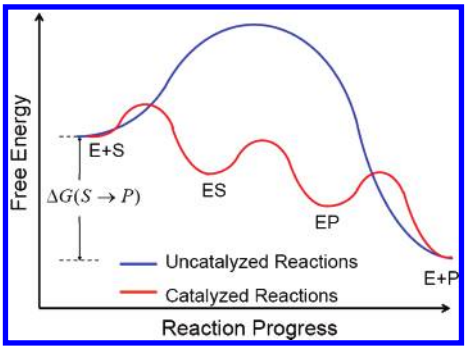

Figure 1. The traditional 1D free energy diagram of enzyme-catalyzed reactions. While the first and third barriers owe their origin to the relevant enzyme conformational change (collectively denoted by the coordinate Q), the second barrier is due to IRC, denoted as X in our treatment of enzymatic reactions. Thus, the reaction coordinate shown here is a mixture of X and Q, reflecting the fact that the activation barrier comes from both the enzyme coordinate Q and IRC X. We have decomposed these two coordinates later.

longer time scales, from milliseconds to 100 s. Interestingly, recent NMR[8−10] and single-molecule[11−13] experiments suggested that conformational fluctuations also occur on the same time scales. Additionally, single-molecule experiments[11−13] have further showed fluctuation at multiple time scales. The very existence of these slow conformational changes on the same time scale of enzymatic reactions makes applications of classic theories of chemical kinetics, namely, transition-state theory (TST) and the Kramers theory,[14] inadequate. This is because a fundamental assumption of these theories is that the bath fluctuation is much faster than the dynamics on the IRC. Such a time scale separation is no longer applicable to proteins, in which the slow conformational fluctuations result in a non-Markovian memory effect.

Many theoretical advances have been made to circumvent the similar non-Markovian behaviors in solution-phase chemical reactions based on a generalized Langevin equation[15] (GLE) description for motion along the IRC, most notably the Grote−Hynes theory.[16] However, in enzyme catalysis, there is no separation of time scale between reactive motion along the IRC and conformational fluctuations. Therefore, implementation of these non-Markovian theories with only a one-dimensional (1D) description of the reaction process along the IRC is still inadequate for proteins.[17,18] Instead of being described by a colored noise term in a GLE, the slow conformational fluctuations should be treated explicitly on an equal footing as the chemical dynamics along the IRC, if one is to reveal the coupling between conformational fluctuation and chemical kinetics.

It is well-known that many enzymatic reactions are enslaved to slow conformational fluctuations. As depicted in Figure 2, for a bond-breaking reaction between atoms A and B, the IRC is denoted by the X coordinate, which is the distance between A and B, and the slow conformational Q coordinate can be the distance between atom B and a nearby atom C, which serves as a catalytic group for this bond-breaking reaction. Only when the Q coordinate reaches certain configuration can the reaction along the X coordinate progress. Because the motion of atom C requires the movement of many other atoms in the enzyme, the motion of this highly collective Q coordinate can be a rate-limiting step for the reaction in many cases.

Here we develop a theory for enzyme-assisted catalysis with a two-dimensional (2D) reaction free energy surface spanned by the IRC, X, and a collective protein conformational coordinate, Q. The free energy surface is obtained by averaging over

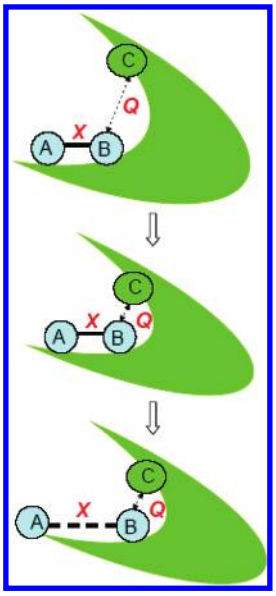

Figure 2. A cartoon illustration of the role of the $X-Q$ pair in enzyme catalysis. X describes the bond distance between atoms A and B, while the slow Q coordinate is the physical distance between the atom B and a nearby amino acid residue C, which serves as the catalytic group for this bond-breaking reaction. Only when the Q coordinate reaches certain configuration can the chemical reaction along the X coordinate progress such that the bond between A and B could break.

all the other degrees of freedom whose motions are assumed to be fast. 2D free energy surfaces have been discussed for specific enzyme behaviors[19] and coupled electron and proton reactions for certain localized areas.[6] Here we construct a 2D free energy surface for the entire catalytic cycle and show how it provides a mechanistic realization of transition-state stabilization.

There are two distinct objectives of this paper:

(1) To formulate a theory based on a general 2D multisurface free energy description of the catalytic process. Because of the involvement of four (primary) states in the MM catalytic process, (i) E···S, unbounded enzyme and substrate contact complex, (ii) ES, bounded enzyme−substrate complex, (iii) EP, bounded enzyme−product complex, and (iv) E···P, unbound enzyme and product contact complex, the relative geometry of the free energy surfaces is a bit complex. These states are represented by displaced harmonic wells whose frequency and relative positions of the minima are characteristics of the four states mentioned above. Substrate binding to enzyme is modeled as a transition from the E···S surface to the ES surface. A reaction zone on the ES surface models the catalysis along the X coordinate. The minima and the reaction positions on the harmonic wells account for the free energy changes involved in each step.

(2) To account for recent experimental observations of multiple-time-scale conformational dynamics and dispersed enzyme kinetics in terms of the above 2D reaction free energy surfaces. The multiple time scales of conformational dynamics are included through a time-dependent diffusion constant, which was obtained from an experimental time correlation function. The propagation on the free energy surface is described by a generalized Smoluchowski equation of the relevant probability density in each surface.

It may now be useful to compare the present theory with a few recent theoretical studies that address the rate of enzymatic reactions. A recent review[7] summarizes the current understanding of various contributing factors within the framework of generalized transition-state theory (GTST). In this framework,

the rate constant of catalysis is a product of an Arrhenius factor (thus accounting for the free energy barrier of activation) and a generalized transmission coefficient (to account for the friction term), which provides the correction from the simple TST. GTST is valid in the limit where enzyme fluctuations do not play a direct dynamical role, and the chemical reaction itself faces a large activation barrier. In other words, this limit where GTST works is exactly opposite to the enzyme dynamics-controlled process discussed above. While enzyme conformational fluctuations reduce the catalysis rate in GTST through the friction term, such fluctuations greatly enhance the rate of catalysis in the present theory.

2. Summary of Relevant Concepts and Observations

We now list some of the well-established concepts and experimental observations that will be included in the present theoretical framework.

(1) Pauling's original thermodynamic insight that "*... the entire and sole source of catalytic power of enzymes is the stabilization of the transition state...*"[20,21] provides a valuable equilibrium picture that articulates the significant lowering of the activation barrier along X. This of course requires averaging over all the degrees of freedom of the enzyme (including Q and all the other enzyme coordinates). The application of catalytic antibody is exactly based on this insight.[22] However, the role of conformational dynamics is beyond this thermodynamic picture.

(2) *Koshland's Concept of "Induced Fit".*[23] After the substrate enters the enzyme active site, the enzyme conformation will rearrange itself so that it helps alignment of the catalytic group with the substrate to lower the activation free energy along the X coordinate. This dynamic view is distinctly different from the static picture of "lock and key".

(3) *Haldane's Concept of Strain Energy Released upon Substrate Binding.*[24] Upon substrate binding, the free energy is used to distort the substrate/enzyme complex in such a way as to facilitate the subsequent reaction. The free energy released allows "conformational strain" to drive the enzyme−substrate complex to the state of low activation barrier for the X coordinate. Molecular motors are examples of using the released free energy to conduct mechanical work in an efficient way.[25]

(4) The concept of gated dynamics[26,27] suggests that conformational fluctuations are often rate-limiting steps for the substrate association.

(5) Recent NMR experimental results show that the enzyme dynamics may play the role of the rate-determining step in the catalytic process.[8−10] For example, in the catalytic activity of hyperthermophilic and mesophilic homologues of adenylate kinase, the critical step is found to be lid-opening.[8] The following are the measured rates of lid-opening ($k_{\mathrm{lid-open}}$) and catalysis: $k_{\mathrm{lid-open}} = 44\ \mathrm{s}^{-1}$ and $k_2 = 50\ \mathrm{s}^{-1}$ for thermoAdk, and $k_{\mathrm{lid-open}} = 286\ \mathrm{s}^{-1}$ and $k_2 = 263\ \mathrm{s}^{-1}$ for mesoAdk.

(6) *Dispersive Protein Dynamics.* Evidence of dispersive protein dynamics comes from a variety of experimental techniques. The pioneering work of Frauenfelder and co-workers has established the dispersed kinetics of rebinding of ligands to hemoglobin and myoglobin upon photodissociation,[28] and the spectral relaxation of the same system was also recorded on time scales ranging from 10^{-12} to 10^{-4} s.[29,30] The existence of long-lived protein conformers was also inferred by mass spectrometry.[31] Recent experiments have further shown that protein dynamics is slow and dispersive at a single-molecule level.[11−13]

(7) *MM Relation Holds Even When the Enzyme Kinetics Is Dispersive.* Real-time monitoring of single-molecule enzymatic turnovers on many enzyme systems[32−37] have unambiguously revealed (a) the multiexponential decay of waiting time distribution of single-enzyme reactions, (b) the existence of strong correlations among the waiting times, and (c) a temporal fluctuation of the single-enzyme turnover rate in the range $10^{-3}-10$ s. Interestingly, the well-known MM relation (eq 1.1) between averaged enzyme velocity and substrate concentration is found to be true, even for these fluctuating enzymes.[36]

3. Formulation of the Theory with 2D Reaction Free Energy Surface of Catalytic Cycle

Here we adopt a coarse-grained statistical mechanical treatment that attempts to capture the central features, and we begin with several initial abstractions and simplifications.

(1) We assume that a natural time scale, τ_{barrier}, can be associated with the barrier crossing dynamics along the X coordinate. This can occur, of course, only at an optimal enzyme configuration (denoted as $Q_{\mathrm{catalysis}}$) that corresponds to the transition state of the X coordinate. This τ_{barrier} appears to range between microseconds to milliseconds,[24] but could be even smaller. In view of this time scale, the normal modes of the enzyme whose influence on the reaction rate is significant can be divided into two groups: those characterized by slower and/or comparable motion, collectively denoted as Q, and those with much faster motions, collectively denoted as $\{1 - Q\}$.

(2) Using the division made above, we construct a set of 2D reaction free energy surfaces formed by X and Q, by averaging all the fast motion of $\{1 - Q\}$.

(3) Using these 2D $X-Q$ reaction free energy surfaces, the general dynamical description of the process can be described by the following reaction−diffusion equation of motion of the joint probability distribution, $\rho_i(X,Q,t)$:

$$\frac{\partial \rho_i(X,Q,t)}{\partial t} = (\Gamma_{Xi} + \Gamma_{Qi})\rho_i(X,Q,t) + \sum_j [k_{ji}(X,Q)\rho_j(X,Q,t) - k_{ij}(X,Q)\rho_i(X,Q,t)] \quad (3.1)$$

where Γ_{Xi} and Γ_{Qi} are the operators that describe (non-Markovian) propagation of population over X and Q on the ith surface, respectively. The precise form of Γ_X (or Γ_Q) is determined by the detailed interaction of X (or Q) with the fast heat bath modes $\{1 - Q\}$. Crossover from the ith surface to the jth is described by a set of reaction windows or funnels, given by $k_{ij}(X,Q)$. Thus, the entire process of catalysis consists of diffusion of the system to the reaction zones, followed by the reaction itself; both are, of course, coupled, then another diffusive process occurs leading to product release. Note that the above equation must conserve the probability of Q as enzyme concentration (probability) and this is done by imposing detailed balance. Later sections of the paper are devoted to the dynamic effects.

We next discuss our selection of states in XQ space.

3.1. Six- versus Four-State Representation of the 2D Reaction Free Energy Surface. Strictly speaking, the whole enzymatic cycle process involves six distinct states: (i) free enzyme and free substrate (E + S) separated by infinite distance; (ii) E and S are close but still unbound (we refer to this as an enzyme−substrate contact pair, E···S); (iii) bound enzyme−substrate complex ES; (iv) bound enzyme−product complex EP; (v) close but unbound enzyme and product contact pair E·

··P; and (vi) free enzyme and free product E + P with infinite distance away.

The diffusion of substrate toward the enzyme in the solution phase is responsible for the transition from fully free state E + S to contact pair state E···S. It is theoretically straightforward and sufficient to treat the dynamics of this process with a three-dimensional (3D) diffusion equation with a general interaction potential between E and S, as in the classic Smoluchowski and Debye theories for diffusion-controlled reactions. The same is again true for the transition from E···P to E + P. In our picture, such substrate/product encounters and dissociations are represented by simple kinetic steps. *We shall thus construct only four-state 2D X−Q reaction free energy surfaces for the enzymatic catalysis process, and neglect states E + S and E + P from the beginning.*

As shown later, such a representation offers considerable generalization of the conventional picture described in Figure 1, which is commonly plotted one-dimensionally.

3.2. General Thermodynamic Construction of Reaction Free Energy Surfaces. The following steps have been followed in the construction of the 2D free energy surfaces:

(1) To be theoretically tractable, we choose all the free energy surfaces $U_I(Q)$ (I = E···S, ES, EP, or E···P) to be harmonic near the equilibrium positions of Q, and also until the crossing point (as in the Kramers theory of activated barrier crossing dynamics). In the single-molecule experiments,[11−13] the free energy surfaces $U_I(Q)$ can *indeed be well approximated by harmonic potentials with angular frequencies* ω_I. Hence, we have

$$U_I(Q) = \frac{1}{2} m\omega_I^2 (Q - Q_{I,e})^2 + U_{I,e} \qquad (3.2)$$

where $Q_{I,e}$ and $U_{I,e}$ are the equilibrium position and equilibrium free energy, respectively.

Note that the free energy surface is expected to be rugged on short time and small length scales, but can be approximated as parabolic on long time and length scales.[38] We shall return to discuss the analogy of some aspects of the present problem with the well-known protein-folding problem.

(2) Because of the chemical potential difference between S and P, the energies of $U_{E\cdots S}(Q)$ and $U_{E\cdots P}(Q)$ differ in free energy by an amount of $\Delta G(S \rightarrow P)$:

$$U_{E\cdots S}(Q) - U_{E\cdots P}(Q) = U_{E\cdots S,e} - U_{E\cdots P,e} = \Delta G(S \rightarrow P) \qquad (3.3)$$

(3) Because of the energetic interaction between enzyme and substrate or product, the equilibrium positions $Q_{I,e}$ for bound states ES and EP are generally different from each other and also different from the positions for unbound states: $Q_{E\cdots S,e} \approx Q_{E\cdots P,e} \neq Q_{ES,e} \neq Q_{EP,e}$. $U_{E\cdots S}(Q)$, $U_{ES}(Q)$, and $U_{EP}(Q)$ are often called displaced harmonic wells.

(4) In order to have closed cycle kinetics, there must exist a transition from E···P back to E···S. Physically, such a process corresponds to the diffusion of P away from E (transition from state E···P to state E + P) and the diffusion of a new substrate S close to E (transition from separated E + S state to contact pair E···S).

On the basis of the above definitions and quantifications in points 1−4, we can now construct free energy surfaces for $U_{E\cdots S}$, U_{ES}, U_{EP}, and $U_{E\cdots P}$. Figure 3 depicts a typical construction represented by a contour plot, and Figure 4 depicts a 3D plot. Figure 5 depicts its projection on enzyme Q coordinate alone.

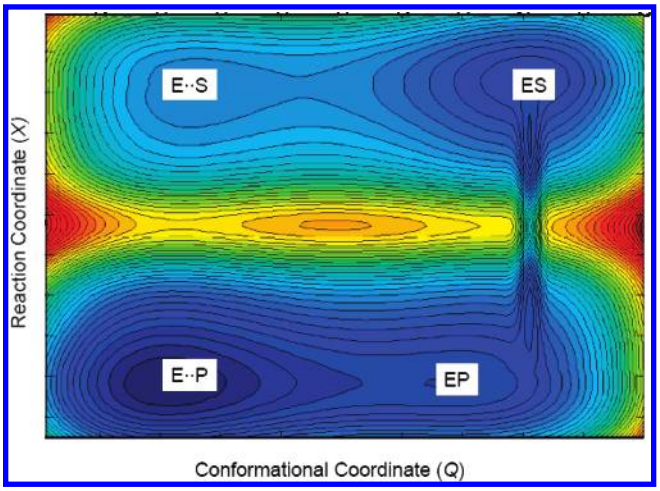

Figure 3. A contour energy diagram of the 2D reaction free energy surfaces of $U_{E\cdots S}$, U_{ES}, U_{EP}, and $U_{E\cdots P}$ in the X and Q planes. The color code (the lower the energy, the deeper the blue) is designed to reflect the relative free energy levels among these four wells (states).

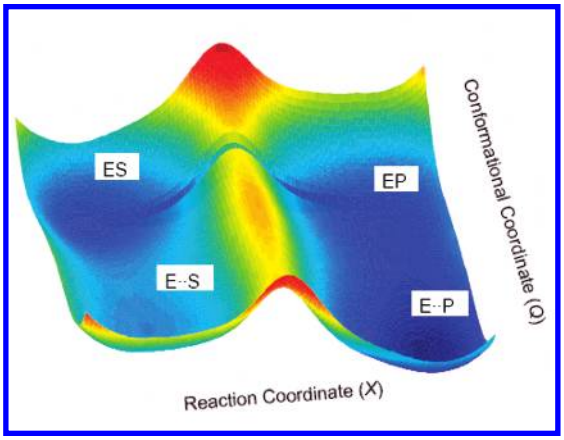

Figure 4. A 3D representation of 2D reaction free-energy surfaces of $U_{E\cdots S}$, U_{ES}, U_{EP}, and $U_{E\cdots P}$. The color bar is designed to reflect the relative free energy levels among these four wells (states). Note the saddle between ES and EP surfaces where efficient reaction along X can take place.

3.3. Substrate Binding and Dissociation. The transition from the unbound, contact pair state E···S to the bound ES state and vice versa, that is, the binding or the dissociation of S to or from E, can be described by a diffusive barrier crossing process in the Q coordinate. As shown in Figure 6, the binding configuration $Q_{binding}$ serves as the dividing surface between the E···S state and the ES state (as in Kramers theory).[14] The energetic quantities such as the equilibrium binding energy $\Delta G^0_{binding}$, the activation energy $\Delta G^{\neq}_{binding}$ for the binding process, and the relaxation energy ΔG_{relax} for the subsequent stabilization process on the *ES* free energy surface are all defined accordingly. Similarly, product release or rebinding can be accounted for by the diffusive dynamics between the bound EP state and the unbound E···P state.

3.4. Transition-State Stabilization Modeled by a Reaction Funnel. Conformational change subsequent to the conversion from the contact pair state E···S to the enzyme−substrate bound ES must lower the activation energy barrier for the X coordinate. This is related to Haldane's concept of strain energy.[24] Although an enzyme has a very large number of possible conformations, the specific and directed nature of the lowering of the activation barrier along X seems to suggest that this work is likely to be accomplished only by a limited number of such conformations. These limited conformations themselves might be connected

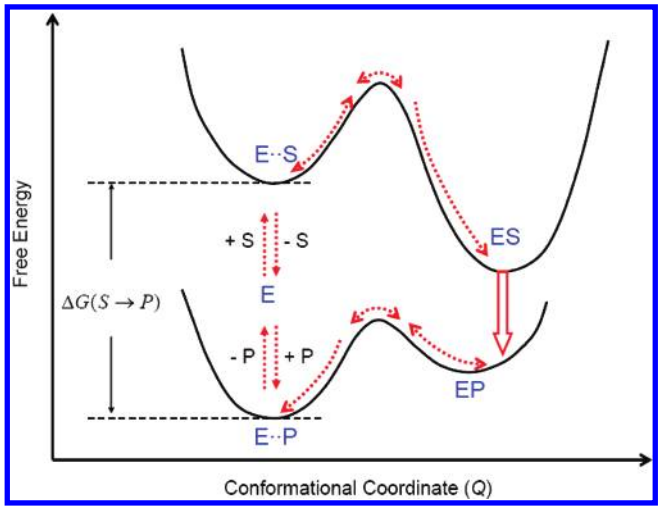

Figure 5. The projection of the 2D reaction free energy surfaces of $U_{E\cdots S}$, U_{ES}, U_{EP} and $U_{E\cdots P}$ onto the enzyme conformation coordinate Q. The "effective" catalysis region of Q is projected as a bar pointing from $U_{ES}(Q)$ to $U_{EP}(Q)$. The red arrows illustrate the "flow" in XQ space for a working enzyme.

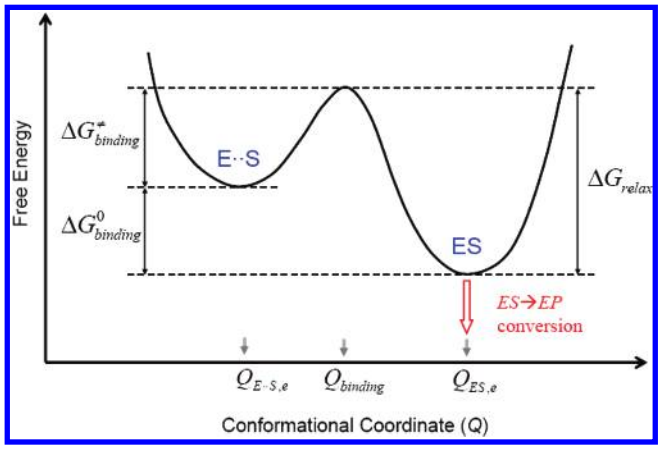

Figure 6. Free energy surface for substrate binding and dissociation. The dividing surface between $U_{E\cdots S}$ and U_{ES} surfaces is the binding configuration of the enzyme substrate complex, denoted as $Q_{binding}$. $\Delta G^0_{binding}$ denotes the equilibrium binding energy, $\Delta G^{\neq}_{binding}$ denotes the binding activation energy, and ΔG_{relax} denotes the relaxation energy for the subsequent stabilization process occurring at the ES surface. These three free energies determine the thermodynamics and kinetics of the enzyme−substrate binding process.

to a broader set of conformations. Hence, we make the following postulate: *only for very limited configurations of Q* (*denoted as* $Q_{catalysis}$) is the stabilization of the activation barrier of X in the ES complex substantial enough that considerable rate acceleration can be achieved compared to that of uncatalyzed reactions.

In order for enzymes to accelerate the rate efficiently, the enzyme conformation Q has to reach that optimal $Q_{catalysis}$ as fast as possible upon substrate binding. This would be difficult and time-consuming if the enzyme conformation has to undergo a random search in the Q space without any free energy bias. We therefore postulate that, a "reaction funnel" should energetically guide the enzyme to the free energy minimum near which $Q_{catalysis}$ is located. Energy gain on increasingly more efficient substrate−enzyme interaction (as Q moves toward $Q_{catalysis}$) is believed to be the driving force for this nonequilibrium downhill relaxation process. This is a situation analogous to the successful "folding funnel" model in protein folding.[39−41] Such a postulation also reflects the notion of "induced fit"[23] and the release of "strain".[25]

3.4.1. Existence of a Catalytic Sink. Following the above postulates, we assume that the Q-dependent catalytic rate constant $k_{IRC}(Q)$ of converting the system from the $U_{ES}(Q)$ surface to the $U_{EP}(Q)$ surface is substantial only for a limited region of Q, and negligible elsewhere. Let us collectively denote the above effective configurations as $Q_{catalysis}$. Thus Q configurations located close to $Q_{catalysis}$ can be considered as the catalysis zone of the enzyme conformation. As postulated, the rate of product conversion, $k_{IRC}(Q)$, will be sharply peaked in this zone. To be mathematically simple, we further assume a Gaussian sink model for $k_{IRC}(Q)$ centered at $Q_{catalysis}$:

$$k_{IRC}(Q) \rightarrow k_{IRC}\frac{1}{\sigma\sqrt{2\pi}}\exp\left[-\frac{(Q-Q_{catalysis})^2}{2\sigma^2}\right] \quad (3.4)$$

A further simplification is obtained by taking the width of the above Gaussian function to approach the limit $\sigma \rightarrow 0$:

$$k_{IRC}(Q) \rightarrow k_{IRC}\delta(Q-Q_{catalysis}) \quad (3.5)$$

We call it a delta-function sink with a finite integrated decay rate constant ($= k_{IRC}$).

Because of the time-scale separation described above, a well-defined rate constant for k_{IRC} is guaranteed in this treatment. Analytically, the magnitude of this k_{IRC} for the X coordinate would be determined through the Grote−Hynes theory[16] with the Q coordinate frozen at $Q_{catalysis}$:

$$k_{IRC} = k^{G-H}(Q = Q_{catalysis}) \quad (3.6)$$

In the Grote−Hynes theory, the interaction between X and fast $\{1-Q\}$ modes gives the corresponding frequency-dependent friction for the diffusive barrier crossing dynamics of X. Such a procedure has been carried out through molecular dynamics simulation.[42] Numerically, one can also run the simulation at the transition state of X, compute the time-dependent transmission coefficient, and record the plateau value.[43,44]

3.4.2. Reaction Funnel Model. In Figures 3, 4, and 5, the $Q_{catalysis}$ zone is shown to be located near the bottom of the $U_{ES}(Q)$ harmonic well. This configuration maximizes the stabilization of the enzyme−substrate complex. To make our theory even simpler and also analytically tractable, we assume that a localized reaction sink is located at the bottom of the harmonic $U_{ES}(Q)$ well, i.e.,

$$Q_{catalysis} \approx Q_{ES,e} \quad (3.7)$$

We believe that this is a realistic limit for most highly evolved enzymes because of its obvious energetic benefits.

Figures 3, 4, and 5 illustrate the energetic coupling between enzyme coordinate Q and IRC X and are largely self-explanatory. The contour plot in Figure 3 shows a narrow region of Q where the activation barrier for the X coordinate is much lower compared to other Q configurations. Such an "effective" region of Q is projected as a bar in Figure 4. Since certain free energy would be released when X progresses to the product side, this will be projected as a free energy drop in the transition from the $U_{ES}(Q)$ to the $U_{EP}(Q)$ surface in Figure 5. The color variation (more blue means lower energy) in the EP and ES wells in Figures 3 and 4 reflects the relative free energy levels. The exact geometric relation between different surfaces is not determined in this work. This will be determined by the energetics of the reactions and requires input from experiments. However, we note that the positions of the well can be rather flexible,

reflecting a large variety of possibilities of many enzyme−substrate systems.

In the following sections, we first describe our theoretical description of enzyme dynamics, followed by a detailed formulation of the catalytic reaction.

4. Enzyme Conformational Reactive Motion: Multiple-Time-Scale Dynamics

Since Q couples directly to the catalytic reaction, we denote, in the spirit of the projection operator technique,[15] the rest of the enzyme conformational coordinates as $\{1 - Q\}$. Thus, interactions between coordinates Q and $\{1 - Q\}$ determine the frictional forces on the relevant conformational fluctuations of the enzyme. Therefore, the role of $\{1 - Q\}$ on the dynamics of Q will be reflected as a general time-dependent diffusion constant, $D(t)$.

We employ a generalized Smoluchowski equation as the equation of motion for the time-dependent probability distribution $\rho_I(Q,t)$[45,46]:

$$\frac{\partial \rho_I(Q,t)}{\partial t} = D_I(t)\left[\frac{m\omega_I^2}{k_B T}\frac{\partial}{\partial Q}(Q - Q_{I,e}) + \frac{\partial^2}{\partial Q^2}\right]\rho_I(Q,t) \qquad (4.1)$$

where $D_I(t)$ is a *time-dependent* diffusion constant related to the normalized time correlation function $C_I(t)$:

$$C_I(t) \equiv \langle Q_I(0)Q_I(t)\rangle / \langle Q_I^2\rangle \qquad (4.2)$$

through

$$D_I(t) = -\frac{k_B T}{m\omega_I^2}\frac{\dot{C}_I(t)}{C_I(t)} \qquad (4.3)$$

In the Makovian limit, $C_I(t)$ is a single-exponential decay, and $D_I(t)$ reduces back to the conventional time-*independent* diffusion constant. However, when $C_I(t)$ is a multiexponential decay and $D_I(t)$ is a decreasing function of time t, more and more friction will be felt as time increases.

As mentioned earlier, recent single-molecule spectroscopic studies of enzyme fluctuations (by measuring the distance fluctuation between a suitably placed donor-acceptor pair inside a protein) have provided quantitative information on $C_I(t)$ for several systems. It is found that it can be fitted to the following form:

$$C_I(t) = \exp(t/t_0)[1 - \mathrm{erf}(\sqrt{t/t_0})] \qquad (4.4)$$

where t_0 is the characteristic time scale of the system, which is ~0.9 s for fluorescein antibody[13] and ~0.07 s for flavin reductase.[11,12] Here we shall use this $C_I(t)$ as an input in our theory. Therefore, the propagation dynamics of $\rho_I(Q,t)$ in eq 4.1 is fully determined by measured $C_I(t)$ through $D_I(t)$. We shall present the numerical result with these measured $C_I(t)$ values in section 7.

The Green function solution of the generalized Smoluchowski equation (eq 4.1) is

$$\rho_I(Q,t|Q_{I,0},0) = \sqrt{\frac{m\omega_I^2}{2\pi k_B T[1 - C_I^2(t)]}} \times \exp\left\{-\frac{m\omega_I^2[(Q - Q_{I,e}) - (Q_{I,0} - Q_{I,e})C_I(t)]^2}{2k_B T[1 - C_I^2(t)]}\right\} \qquad (4.5)$$

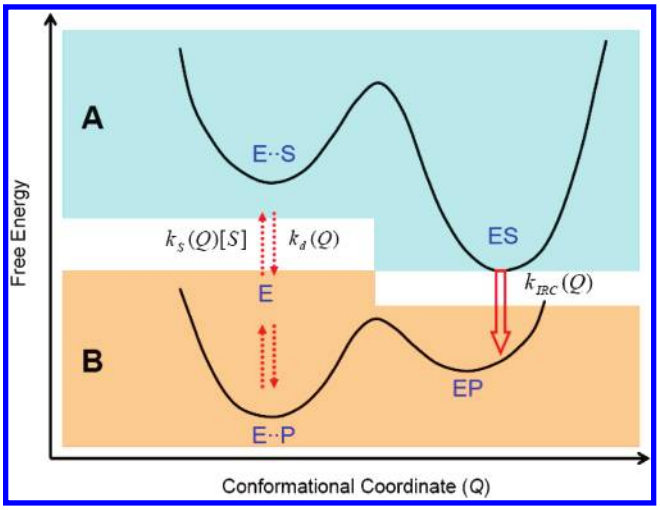

Figure 7. Quasi-equilibrium limit for MM relation. E···S and ES surfaces together are denoted as A, and E···P and *EP* surfaces and free E together are denoted as B.

under the initial condition $\rho_I(Q,t = 0) = \delta(Q - Q_{I,0})$. On the basis of eq 4.5, one can analytically track the evolution of the system once the initial condition and dynamics of $C_I(t)$ are known.

5. A General Theory of MM Kinetics in The Presence of Dispersed Kinetics

We demonstrate in this section that the general MM relation between the steady-state catalysis velocity and the substrate concentration can still hold in the presence of dispersed multi-time-scale kinetics of protein conformational dynamics, under both quasi-equilibrium conditions and quasi-static conditions. Therefore, the theory reconciles these two widely observed phenomena, which has been experimentally demonstrated in single-molecule studies on β-galactosidase.[36] The present formalism is an extension of an earlier theoretical study.[47]

5.1. Quasi-equilibrium Limit. We group the free energy surfaces E···S and ES together and denote them as A, and we group E···P and EP surfaces as well as free E together and denote them as B. Such a characterization is illustrated in Figure 7 . The general master equation for the dynamics of transitions between A and B groups can be written formally as

$$\frac{\partial}{\partial t}\begin{pmatrix}\rho_A(Q,t)\\ \rho_B(Q,t)\end{pmatrix} = \begin{pmatrix}\Gamma_A - k_d(Q) - k_{IRC}(Q) & k_S(Q)[S]\\ k_d(Q) + k_{IRC}(Q) & \Gamma_B - k_S(Q)[S]\end{pmatrix}\begin{pmatrix}\rho_A(Q,t)\\ \rho_B(Q,t)\end{pmatrix} \qquad (5.1)$$

where $\rho_A(Q,t)$ and $\rho_B(Q,t)$ are the time- and Q-dependent probabilities of the enzyme being in group A and B, respectively, Γ_A is the general diffusion operator in A, Γ_B is the general diffusion operator in B, k_S is the classic Smoluchowski diffusion rate constant forming the E···S encounter complex (shown in Figure 5), k_d is the dissociation rate constant of the encounter complex (also shown in Figure 5), and $k_{IRC}(Q)$ is the catalytic conversion rate constant of the Q-dependent sink.

We now require that, in the absence of $k_S(Q)$, $k_d(Q)$, and $k_{IRC}(Q)$, eq 5.1 correctly describes the relaxation to the equilibrium Boltzmann distribution, $\exp[-U(Q)/k_B T]$. Since the equilibrium

distribution must be stationary (i.e., its time derivative is zero), we have

$$\begin{pmatrix}\Gamma_A & 0\\ 0 & \Gamma_B\end{pmatrix}\begin{pmatrix}\exp[-U_A(Q)/k_BT]\\ \exp[-U_B(Q)/k_BT]\end{pmatrix}=0 \tag{5.2}$$

Equations 5.1 and 5.2 complete the description of the dynamics.

We next consider the steady-state solution of eq 5.1. The steady-state probabilities $\rho_A^{ss}(Q)$ and $\rho_B^{ss}(Q)$ satisfy

$$\begin{pmatrix}\Gamma_A - k_d(Q) - k_{IRC}(Q) & k_S(Q)[S]\\ k_d(Q) + k_{IRC}(Q) & \Gamma_B - k_S(Q)[S]\end{pmatrix}\begin{pmatrix}\rho_A^{ss}(Q)\\ \rho_B^{ss}(Q)\end{pmatrix}=0 \tag{5.3}$$

along with the normalization condition

$$\int(\rho_A^{ss}(Q)+\rho_B^{ss}(Q))dQ=1 \tag{5.4}$$

The steady-state enzymatic velocity, which is equal to the average number of turnovers per unit time per enzyme (or to the reciprocal of the mean time between successive catalytic events), is given by

$$v=\int k_{IRC}(Q)\,\rho_A^{ss}(Q)\,dQ \tag{5.5}$$

In the limit of fast enzyme conformational dynamics and slow catalysis sink, the effects of diffusion operators Γ_A and Γ_B are much larger than that of $k_{IRC}(Q)$. Equation 5.3 can be simplified into the following expression:

$$\begin{pmatrix}\Gamma_A - k_d(Q) & k_S(Q)[S]\\ k_d(Q) & \Gamma_B - k_S(Q)[S]\end{pmatrix}\begin{pmatrix}\rho_A^{ss}(Q)\\ \rho_B^{ss}(Q)\end{pmatrix}=0 \tag{5.6}$$

Using the ansatz

$$\begin{pmatrix}\rho_A^{ss}(Q)\\ \rho_B^{ss}(Q)\end{pmatrix}=\begin{pmatrix}\alpha\exp[-U_A(Q)/k_BT]\\ \beta\exp[-U_B(Q)/k_BT]\end{pmatrix}$$

we have the following condition:

$$\begin{pmatrix}\Gamma_A - k_d(Q) & k_S(Q)[S]\\ k_d(Q) & \Gamma_B - k_S(Q)[S]\end{pmatrix}\times\begin{pmatrix}\alpha\exp[-U_A(Q)/k_BT]\\ \beta\exp[-U_B(Q)/k_BT]\end{pmatrix}=0 \tag{5.7}$$

Together with eq 5.2, this allows us to write the following relation:

$$\begin{pmatrix}-k_d(Q) & k_S(Q)[S]\\ k_d(Q) & -k_S(Q)[S]\end{pmatrix}\begin{pmatrix}\alpha\exp[-U_A(Q)/k_BT]\\ \beta\exp[-U_B(Q)/k_BT]\end{pmatrix}=0 \tag{5.8}$$

which now leads to the following relation:

$$\frac{\alpha\exp[-U_A(Q)/k_BT]}{\beta\exp[-U_B(Q)/k_BT]}=\frac{k_S(Q)[S]}{k_d(Q)} \tag{5.9}$$

Now note that, in our free energy surfaces, in the effective region of $Q \le Q_{release}$, both the left-hand side and right-hand side of above equation are independent of Q!

We now substitute the ansatz, together with eq 5.9, into eq 5.4, and solve for the constant α to obtain

$$\alpha=\frac{k_S[S]}{k_S[S]+k_d}\frac{1}{\int e^{-U_A(Q)/k_BT}\,dQ} \tag{5.10}$$

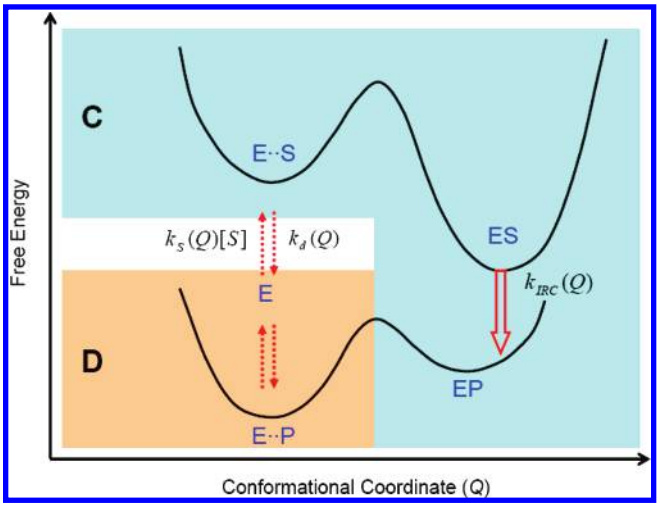

Figure 8. Quasi-static condition for MM relation. E···S, ES, and EP surfaces together are denoted as C, and E···P surface and E together are denoted as D.

Therefore, the steady-state probability is given by

$$\rho_A^{ss}(Q)=\frac{k_S[S]}{k_S[S]+k_d}\frac{e^{-U_A(Q)/k_BT}}{\int e^{-U_A(Q)/k_BT}\,dQ} \tag{5.11}$$

The steady-state enzymatic velocity has the desirable MM form

$$v=\frac{\chi_2[S]}{[S]+C_M} \tag{5.12}$$

where the apparent catalytic rate (χ_2) and the apparent Michaelis constant (C_M) are given by

$$\chi_2=\frac{\int k_{IRC}(Q)e^{-U_A(Q)/k_BT}\,dQ}{\int e^{-U_A(Q)/k_BT}\,dQ},\ C_M=k_d/k_S \tag{5.13}$$

5.2. Quasi-static Condition. We now consider the limiting case where the motion on the E···P surface is essentially static. Thus, the diffusion on E···P and EP surfaces is very slow. We now regroup the free energy surfaces: we group the E···S, ES, and EP surfaces together and denote them as C, and group the E···P surface and E together and denote them as D. Such a grouping is illustrated in Figure 8.

We now write the general master equation as

$$\frac{\partial}{\partial t}\begin{pmatrix}\rho_C(X,Q,t)\\ \rho_D(X,Q,t)\end{pmatrix}=\begin{pmatrix}\Gamma_C - k_d(Q) & k_S(Q)[S]\\ k_d(Q) & \Gamma_D - k_S(Q)[S]\end{pmatrix}\begin{pmatrix}\rho_C(X,Q,t)\\ \rho_D(X,Q,t)\end{pmatrix} \tag{5.14}$$

where $\rho_C(X,Q,t)$ is the probability of the enzyme being at C, $\rho_D(X,Q,t)$ is the probability of the enzyme being at D, Γ_C is the general diffusion plus reaction operator in C, and Γ_D is the general diffusion operator in D. Note that the Q-dependent sink $k_{IRC}(X,Q)$ is included in the Γ_C term.

Again, we solve for the equilibrium solution as

$$\begin{pmatrix}\Gamma_C & 0\\ 0 & \Gamma_D\end{pmatrix}\begin{pmatrix}\exp[-U_C(X,Q)/k_BT]\\ \exp[-U_D(X,Q)/k_BT]\end{pmatrix}=0 \tag{5.15}$$

The steady-state probabilities must satisfy the following condition:

$$\begin{pmatrix} \Gamma_C - k_d(Q) & k_S(Q)[S] \\ k_d(Q) & \Gamma_D - k_S(Q)[S] \end{pmatrix} \begin{pmatrix} \rho_C^{ss}(X,Q) \\ \rho_D^{ss}(X,Q) \end{pmatrix} = 0 \quad (5.16)$$

and the normalization condition

$$\int (\rho_C^{ss}(X,Q) + \rho_D^{ss}(X,Q)) dX dQ = 1 \quad (5.17)$$

The steady-state enzymatic velocity is now given by

$$\nu = \int k_{IRC}(X,Q)\rho_C^{ss}(X,Q) dX dQ \quad (5.18)$$

The sum of the two equations given in eq 5.16 gives

$$\Gamma_C \rho_C^{ss}(X,Q) + \Gamma_D \rho_D^{ss}(X,Q) = 0 \quad (5.19)$$

When the E···P surface is essentially static in Q, we can set

$$\Gamma_D = 0 \quad (5.20)$$

It then follows that

$$\Gamma_C \rho_C^{ss}(X,Q) = 0 \quad (5.21)$$

Hence $\rho_C^{ss}(X,Q)$ must be proportional to $\exp[-U_C(X,Q)/k_BT]$ as a result of eq 15. Using the ansatz

$$\rho_C^{ss}(X,Q) = \gamma \exp[-U_C(X,Q)/k_BT] \quad (5.22)$$

in eq 5.16 together with $\Gamma_D = 0$, we have

$$\rho_D^{ss}(X,Q) = \frac{k_d(Q)}{k_S(Q)[S]} \gamma \exp[-U_3(X,Q)/k_BT] \quad (5.23)$$

Use of both eqs 5.22 and 5.23 in eq 5.17 leads to an expression for the constant γ. Thus, together with eq 5.20, $\rho_C^{ss}(X,Q)$ is given by

$$\rho_C^{ss}(X,Q) = \frac{e^{-U_C(X,Q)/k_BT}}{\left(1 + \frac{1}{[S]}\frac{k_d}{k_S}\right)\left(\int e^{-U_C(X,Q)/k_BT} dX dQ\right)} \quad (5.24)$$

The steady-state enzymatic velocity is, therefore, given by

$$\nu = \frac{\int k_{IRC}(X,Q) e^{-U_C(X,Q)/k_BT} dX dQ}{\left(1 + \frac{1}{[S]}\frac{k_d}{k_S}\right)\left(\int e^{-U_C(X,Q)/k_BT} dX dQ\right)} \quad (5.25)$$

Therefore, the apparent catalytic rate (χ_2) and apparent Michaelis constant (C_M) are given by

$$\chi_2 = \frac{\int k_{IRC}(X,Q) e^{-U_C(X,Q)/k_BT} dX dQ}{\int e^{-U_C(X,Q)/k_BT} dX dQ}, \; C_M = \frac{k_d}{k_S} \quad (5.26)$$

This completes our demonstration that the MM expression holds even with dispersive kinetics under quasi-static conditions.

6. Enzyme Catalysis: First-Passage Time Distribution of Turnover

Let us now consider a scenario that could be applicable to many enzymes: large-scale enzyme conformational rearrangement occurs after the substrate enters the active site but before the catalytic sink zone is reached so that the conformational relaxation from $Q = Q_{binding}$ to $Q_{catalysis}$ and the subsequent conversion from ES to EP for the X coordinate become the rate-limiting steps of the entire catalytic cycle. Figure 9 depicts the underlying reaction free energy surfaces for such a generic case in which the activation energy $\Delta G^{\neq}_{binding}$ for the binding is negligible, reflecting Haldane's notion of "immediate free energy release of conformational strain upon substrate binding". For example, many ATP-driven enzymes[48] and DNA/RNA polymerases[49] are believed to satisfy such a scenario. We shall discuss several limiting cases where the first-passage time distribution of the catalytic reaction can be analytically calculated. Through these limiting cases, we hope that some aspects of the role of conformational dynamics in reaction dynamics can be made transparent.

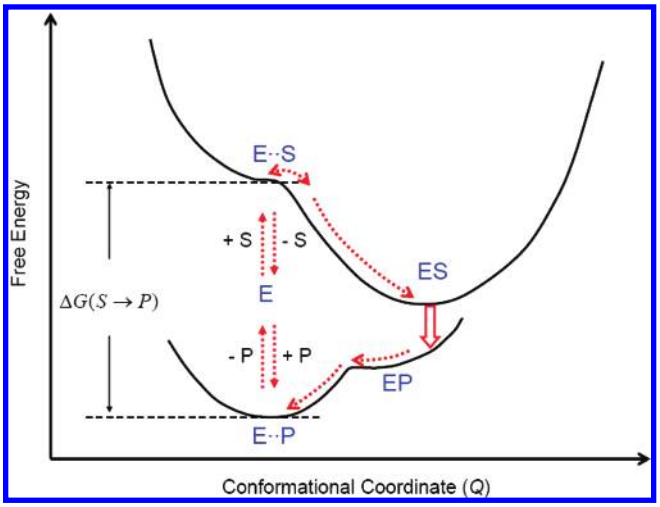

Figure 9. Reaction free-energy surfaces with negligible binding activation energy $\Delta G^{\neq}_{binding}$. When the enzyme is saturated with substrate concentration, $\Delta G^{\neq}_{binding}$ is small, and the product release is also relatively fast, then the conformational relaxation from $Q_{binding}$ to $Q_{catalysis}$ and the subsequent conversion from ES to EP for the X coordinate become the rate-limiting steps of the whole enzymatic cycle.

$Q_{binding}$ is the enzyme conformation where the substrate binding occurs, determined by the dividing surface between $U_{E\cdots S}(Q)$ and $U_{ES}(Q)$ (as shown in Figures 3−6). Therefore, it serves as the initial condition of $\rho_{ES}(Q,t=0)$:

$$\rho_{ES}(Q,t=0) = \delta(Q - Q_{binding}) \quad (6.1)$$

We also set reflection barriers at infinite values of Q, $\rho_{ES}(Q = \pm\infty,t) = 0$. The first-passage time distribution $f(t)$ is the negative time derivative of the survival probability $S(t)$:

$$f(t) = -\frac{d}{dt} S(t) \quad (6.2)$$

According to the relative magnitude of the conformational time scales and the catalysis rate of the delta-function sink, we have two limiting cases, each of which allows for analytic solutions for the first-passage time distribution.

6.1. Slow Catalysis Sink. When the time scale of conformational dynamics is much faster than that of the time constant of the decay from the sink (given by $1/k_{IRC}$), the local equilibrium in the potential well, $U_{ES}(Q)$, is always maintained, even when the catalysis is going on, and the rate-limiting step is the catalysis itself. Thus, the survival probability follows a simple first-order rate process:

$$S(t) = \exp(-k_{IRC}t) \tag{6.3}$$

and the first-passage time distribution is also a single-exponential decay in time:

$$f(t) = k_{IRC}\exp(-k_{IRC}t) \tag{6.4}$$

Obviously, $f(t)$ is independent of the fast conformational dynamics of the enzyme. This is the limit that corresponds to IRC-controlled enzymes where the slow sink rate determines the entire enzyme reaction dynamics.

6.2. Fast Catalysis Sink. When the rate of the catalysis (= k_{IRC}) is much faster than any characteristic time scale of diffusion (for example, from the initial $Q_{binding}$ to the final sink at $Q_{catalysis}$ (= $Q_{ES,e}$)), the delta-function sink with finite decay rate can be treated as a pinhole sink with instantaneous death, which is essentially an absorption barrier boundary at the origin

$$\rho_{ES}(Q = Q_{ES,e},t) = 0 \tag{6.5}$$

which holds for all times.

In this limit, one can find the analytic expression for $\rho_{ES}(Q,t)$ at all times by using the method of images and the Green's function of the non-Markovian diffusion operator. The resultant final expression is given by

$$\rho_{ES}(Q,t) = \left(\frac{m\omega_{ES}^{\,2}}{2\pi k_B T[1 - C_{ES}^{\,2}(t)]}\right)^{1/2} \times \left\{\exp\left(-\frac{m\omega_{ES}^{\,2}[(Q - Q_{ES,e}) - (Q_{binding} - Q_{ES,e})C_{ES}(t)]^2}{2k_B T[1 - C_{ES}^{\,2}(t)]}\right) - \exp\left(-\frac{m\omega_{ES}^{\,2}[(Q - Q_{ES,e}) + (Q_{binding} - Q_{ES,e})C_{ES}(t)]^2}{2k_B T[1 - C_{ES}^{\,2}(t)]}\right)\right\} \tag{6.6}$$

The survival probability $S(t)$ is obtained by an integration of $\rho_{ES}(Q,t)$ with respect to Q:

$$\begin{aligned} S(t) &= \int_{Q_{ES,e}}^{\infty} dQ\,\rho_{ES}(Q,t) \\ &= \left(\frac{m\omega_{ES}^{\,2}}{2\pi k_B T[1 - C_{ES}^{\,2}(t)]}\right)^{1/2} \times \int_0^{\infty} dQ \left(\exp\left\{-\frac{m\omega_{ES}^{\,2}[Q - (Q_{binding} - Q_{ES,e})C_{ES}(t)]^2}{2k_B T[1 - C_{ES}^{\,2}(t)]}\right\} - \exp\left\{-\frac{m\omega_{ES}^{\,2}[Q + (Q_{binding} - Q_{ES,e})C_{ES}(t)]^2}{2k_B T[1 - C_{ES}^{\,2}(t)]}\right\}\right) \\ &= \mathrm{erf}[F(t)] \end{aligned} \tag{6.7}$$

where $F(t)$ is

$$F(t) = \left(\frac{m\omega_{ES}^{\,2}(Q_{binding} - Q_{ES,e})^2}{2k_B T}\frac{C_{ES}^{\,2}(t)}{1 - C_{ES}^{\,2}(t)}\right)^{1/2} \tag{6.8}$$

the error function, erf a, is defined as $\mathrm{erf}\ a = (2/\sqrt{\pi})\int_0^a dy\ \exp(-y^2)$.

With the defined expression of the relaxation energy ΔG_{relax} for the stabilization subsequent to binding to the ES surface in Figure 6, we can have a simplified expression for $F(t)$:

$$F(t) = \left(\frac{\Delta G_{relax}}{k_B T}\frac{C_{ES}^{\,2}(t)}{1 - C_{ES}^{\,2}(t)}\right)^{1/2} \tag{6.9}$$

The corresponding first-passage time distribution is given by

$$f(t) = \frac{-2}{\sqrt{\pi}}\exp[-F^2(t)]F'(t) \tag{6.10}$$

Hence, the reaction dynamics is completely determined by the thermodynamic ΔG_{relax} and the conformational dynamics $C_{ES}(t)$, through eqs 6.9 and 6.10.

This is the limit where the catalysis reaction is so much evolved (or optimized) that the protein conformational dynamics totally determines the enzyme reaction dynamics, which is similar to the solvent-controlled electron transfer discussed by Hynes,[46] Barbara,[50] and Zusman[51] et al., among many others. Numerical results for a specific enzyme case will be presented in the following section.

6.3. Intermediate Catalysis Sink. While analytical solution can be obtained for each of the two limiting cases discussed above, the same is not true for the general case which requires numerical solution. However, some insight into the nature of survival probability can still be obtained when the time-scale separation exists. In such a scenario, we can exploit the two limiting conditions analyzed above and obtain an approximate solution.

To illustrate the basic idea, we employ simple biphasic relaxation kinetics of the enzyme conformational dynamics,

$$C_{ES}(t) = (1/2)\exp\left(-\frac{t}{\tau_f}\right) + (1/2)\exp\left(-\frac{t}{\tau_S}\right) \tag{6.11}$$

where the two decay time scales are assumed to be well separated, i.e.,

$$\tau_f \ll \tau_S \tag{6.12}$$

Such $C_{ES}(t)$ represents one of the simplest non-trivial cases of non-Markovian dynamics and only partly mimics the vast range of time scales observed in enzyme conformation dynamics.

The strategy is to utilize the time-scale separation of the biphasic conformational dynamics to treat the delta-function sink as giving rise to a first-order rate process for the component of fast diffusion dynamics, while treating the slow diffusion as facing an absorption barrier boundary with instantaneous death. The fact that such a technique can be partially successful is clear from the Green function of the diffusion, which changes sharply at short times as a result of the fast component of $C_{ES}(t)$.

In the presence of time-scale separation between the two components $\tau_f \ll \tau_S$, the biphasic $C_{ES}(t)$ in eq 6.11 has a plateau value of 1/2 at a intermediate time scale $\tau^*(\tau_f \ll \tau^* \ll \tau_S)$. The corresponding $S(t)$ given in eq 6.7 also reaches a plateau value S^*:

$$S^* = \mathrm{erf}\left[\sqrt{\frac{\Delta G_{relax}}{3k_B T}}\right] \tag{6.13}$$

Obviously, the larger ΔG_{relax} is, the larger the plateau survival probability S^* is.

On the basis of the plateau value S^* given in eq 6.13, we modify the fast portion of the survival probability $S(t)$ given in eq 6.7 into the first-order rate process given in eq 6.3, while leaving the slow portion of $S(t)$ unchanged. We can, therefore,

adopt the following hybridized expression:

$$S(t) \approx \begin{cases} S^* + (1 - S^*)\exp(-k_{IRC}t) & t < \tau^* \\ \mathrm{erf}[F(t)] & t \geq \tau^* \end{cases} \quad (6.14)$$

Again, because of the time-scale separation $\tau_f \ll 1/k_{IRC} \ll \tau^*$, both short-time and long-time expressions of $S(t)$ approach S^* at τ^*, allowing a smooth junction of the two functions.

Therefore, the resulting $f(t)$ is given by

$$f(t) \approx \begin{cases} (1 - S^*)k_{IRC}\exp(-k_{IRC}t) & t < \tau^* \\ \frac{-2}{\sqrt{\pi}}\exp[-F^2(t)]F'(t) & t \geq \tau^* \end{cases} \quad (6.15)$$

As one expects, the farther the $Q_{binding}$ is from the $Q_{ES,e}$, the smaller the component of the fast single exponential is in the overall first-passage time distribution.

7. Numerical Results and Comparison with Single-Molecule Experiments

Here we first explore several aspects of the fast catalysis limit numerically using the assumption of simple Markovian protein conformational dynamics. Subsequently, the observed non-Markovian conformational dynamics is incorporated to calculate the first-passage time distribution of catalysis. We have compared theoretical predictions with experimental results on the catalysis turnover dynamics of single-molecule lipase B.[34]

7.1. Illustration with Markovian Conformational Dynamics. If we assume that the protein conformational dynamics is a single-exponential decay with time constant τ

$$C_{ES}(t) = \exp(-t/\tau) \quad (7.1)$$

then the resulting expressions for survival probability $S(t)$ and mean first-passage time distribution $f(t)$ are given by the following expressions:

$$S(t) = \mathrm{erf}\left[\left(\frac{\Delta G_{relax}}{k_B T}\frac{\exp(-2t/\tau)}{1 - \exp(-2t/\tau)}\right)^{1/2}\right] \quad (7.2)$$

$$f(t) = \frac{2}{\sqrt{\pi}\,\tau}\frac{k_B T}{\Delta G_{relax}}\left[\frac{\Delta G_{relax}}{k_B T}\frac{1}{\exp(2t/\tau) - 1}\right]^{3/2} \times \exp\left[\frac{\Delta G_{relax}}{k_B T}\frac{\exp(-2t/\tau)}{\exp(-2t/\tau) - 1} + \frac{2t}{\tau}\right] \quad (7.3)$$

respectively.

Figure 10a,b shows the time dependence of $S(t)$ and $f(t)$ for three different values of $\Delta G_{relax}/k_B T$ (0.1, 1, and 10), under the same time constant of conformational dynamics, $\tau = 1$. Slower overall reaction is expected as the relaxation energy $\Delta G_{relax}/k_B T$ becomes larger. At longer times, that is, when $t/\tau \gg 1$, all three decay curves become single exponential. Note that the long-time decay rates are the same for all three curves, because they share the same conformational dynamics. Figure 10 can also be regarded as a depiction of the temperature dependence of the dynamics of the reaction.

Figure 11a,b shows $S(t)$ and $f(t)$ for three different time constants of conformational dynamics ($\tau = 0.2$, 1, and 5) with the same $\Delta G_{relax} = k_B T$. Slower overall reaction is expected as the conformational dynamics gets slower (larger time constant τ). Again, at long times, all three decay curves become single exponential. However, in contrast to the previous case (depicted in Figure 10), now the three curves exhibit different long-time decay rates due to distinct time scales of conformational

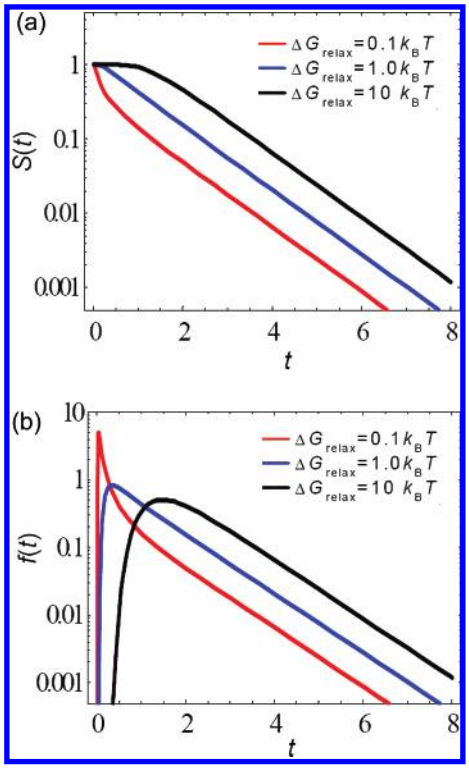

Figure 10. (a) The time dependence of the survival probability $S(t)$, and (b) the first-passage time distribution $f(t)$, for Markovian conformational dynamics in the limit of fast catalysis sink, evaluated through eqs 7.1−7.3. Three different relaxation energies $\Delta G_{relax}/k_B T$ are shown: 0.1 (red), 1 (blue), and 10 (black). All the curves have been calculated with the same time constant of conformational dynamics, $\tau = 1$. This plot can also be interpreted as depicting the temperature dependence of the catalytic dynamics.

dynamics. Since the time constant τ is proportional to the solvent viscosity imposed on the Q coordinate, Figure 11 can also be regarded as demonstrating the viscosity dependence of the reaction.

7.2. Comparison to Single-Molecule Experiments. As noted earlier, single-molecule experiments have successfully measured detailed conformational dynamics $C_{ES}(t)$ for several protein and enzyme systems, and over more than four decades of time. It is found that a time correlation function that characterizes conformational fluctuations can be fitted rather well to the following form:

$$C_{ES}(t) = \exp(t/t_0)[1 - \mathrm{erf}(\sqrt{t/t_0})] \quad (7.4)$$

where t_0 is the characteristic time scale of the protein system: ~0.9 s for fluorescein antibody,[13] and ~0.07 s for flavin reductase.[11,12] We need this $C_{ES}(t)$ as an input in our theory. The frequencies of the harmonic surfaces for the above enzyme and protein systems have already been computed and found to be equal to

$$U_{ES}(Q) \approx \frac{k_B T Q^2}{2\theta} \quad (7.5)$$

where $\theta = k_B T/m\omega^2$ is about 0.2 Å^2. Note that these are all experimentally measured quantities. These numbers are expected to vary from system to system, but one should be able to place certain realistic bounds on the parameter space. For example, t_0 should be less than a second but more than a millisecond. The displacement $Q_{binding} - Q_{ES,e}$ should be less than 1 Å because this is an effective displacement. If we know the free

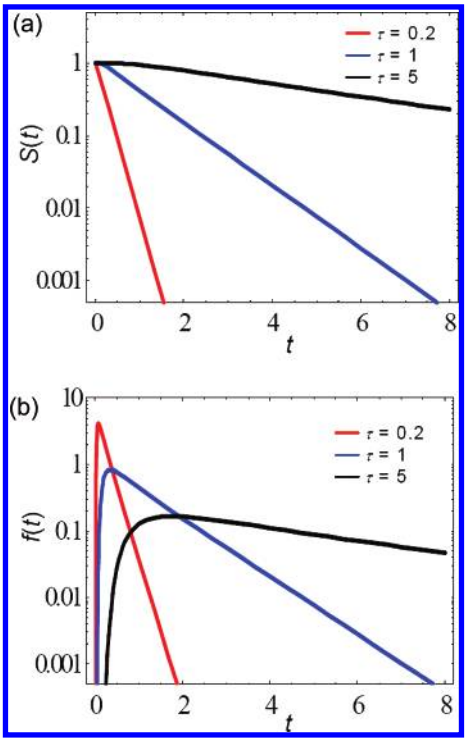

Figure 11. (a) The survival probability $S(t)$, and (b) the first-passage time distribution $f(t)$ for Markovian conformational dynamics in the fast catalysis sink, evaluated through eqs 7.1−7.3. We have used three different time constants of conformational dynamics: $\tau = 0.2$ (red), 1 (blue), and 5 (black), but the same relaxation energy $\Delta G_{relax} = k_B T$. This plot can also be interpreted as depicting the viscosity dependence of the dynamics.

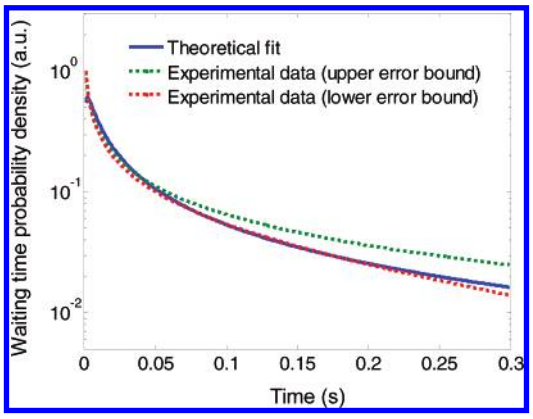

Figure 12. The first-passage time distribution of the enzyme reaction funnel model in the fast catalysis sink limit, predicted with the enzyme conformational time correlation function given by eq 7.4. The theoretical $f(t)$ quantitatively reflects the nature of multiexponential decay measured in recent single-molecule experiments on lipase B, which is slow enough to allow for real-time monitoring under saturated substrate concentration.[34] The theoretical fitted quantities are $Q_{binding} - Q_{ES,e} \sim 0.4$ Å, and conformational dynamics $t_0 \sim 0.7$ s in $C_{ES}(t)$ in eq 7.4. The orders-of-magnitude of the fitted parameters are rather reasonable. The upper and lower error bounds of the experimental result are calculated from data presented in ref 34, which can be fitted by a empirical function: $\exp[-(t/\tau)^{\alpha}]$, where $\tau = 1.15$ μs and $\alpha = 0.15$.

energy of stabilization, then we can easily estimate $Q_{binding} - Q_{ES,e}$, especially when the effective frequency can be obtained from single-molecule experiments.

We now apply the above scheme to real catalytic turnover dynamics, i.e., that of lipase B. Single-molecule experimental results of this reaction have been reported recently by the group of de Schryver and Hofkens.[34] As shown in Figure 12, the theoretical $f(t)$, evaluated from eqs 6.9 and 6.10, can indeed

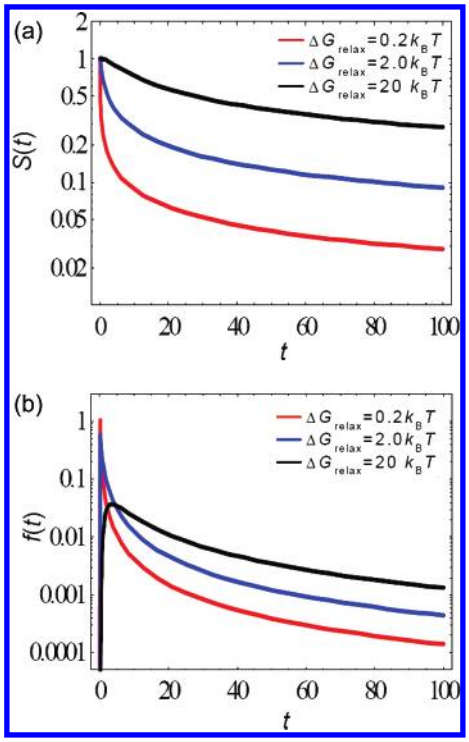

Figure 13. (a) The survival probability $S(t)$, and (b) the first-passage time distribution $f(t)$ for non-Markovian conformational dynamics in the fast catalysis sink. Calculations have been performed for three different relaxation energies $\Delta G_{relax}/k_B T$: 0.2 (red), 2 (blue) and 20 (black), but using the same protein conformational dynamics (using reduced unit $t_0 = 1$) given by eq 7.4. With everything else being the same, smaller (or larger) relaxation energy gives more (or less) dispersed kinetics. This implies that the dispersed dynamics may not be very apparent for large relaxation energy.

quantitatively fit the waiting time distribution of single-molecule lipase B, which was measured under saturated substrate concentration.[34,35] Note that we have essentially performed a two-parameter fitting procedure: $Q_{binding} - Q_{ES,e} \sim 0.4$ Å, which corresponds to thermodynamic $\Delta G_{relax} \sim 0.35 k_B T$ by utilizing experimentally measured frequency as given by eq 7.5, and conformational dynamics $t_0 \sim 0.7$ s in $C_{ES}(t)$ in eq 7.4. The theoretical estimate of the magnitude of $Q_{binding} - Q_{ES,e} \sim 0.4$ Å is quite reasonable, and the conformational dynamics correlation time constant $t_0 \sim 0.7$ s is also quite close to the measured value of ~0.9 s for fluorescein antibody.[13] *Therefore, the reaction funnel with the delta-function sink model establishes a theoretical connection between the multi-time-scale conformational dynamics and dispersive catalytic reaction dynamics of an enzyme.* To the best of our knowledge, such a connection is provided here from a free energy surface perspective for the first time.

Since the overall rate of dispersed enzyme dynamics depends strongly on the magnitude of relaxation energy, we have shown in Figure 13a,b the decay behavior of $S(t)$ and $f(t)$ for three different $\Delta G_{relax}/k_B T$ (0.2, 2, and 20) with the same decay time constant t_0 (reduced unit $t_0 = 1$ in eq 7.4). With everything else remaining the same, the smaller (or the larger) relaxation energy gives rise to the more (or less) dispersed kinetics. This implies that the dispersed dynamics may not be observed for large relaxation energy. This is an interesting (and new) result.

8. Enzyme Diversity and the Broad Parameter Space

Dynamics of enzymatic catalysis are known to exhibit a considerable degree of diversity for different enzymatic reac-

tions. The present theory accounts for this diversity in terms of a broad parameter space, which allows for important *specific* (to a given individual enzymatic reaction) features, even in this coarse-grained description.

In fact, such diversity and specificity are reflected from many perspectives of the theoretical formalism. First and foremost, the rate-limiting step can be either a single process or a combination of the following processes: (i) substrate diffusion at low concentrations, (ii) enzyme conformational activation for substrate binding, (iii) enzyme conformational relaxation after substrate binding (induced fit), (iv) catalytic reaction along IRC, and (v) product release. In sections 6 and 7, we have focused on the dynamics of catalysis subsequent to binding and the IRC catalysis. If the dynamics of binding of S to E is activated, then that might be the rate-determining step. We shall discuss elsewhere a different scenario.[52] Second, the frequencies of the E···S, ES, EP, and E···P surfaces are expected to vary for different enzymatic reactions. These can be and have been measured in single-molecule experiments, reflecting the rigidity of the reactive motion, which will determine the activation and relaxation energy. Third, the relative positions of E···S and ES and of ES and EP harmonic well potentials in Q space are determined by the energetics and thermodynamic driving force of the reaction. Fourth, the catalytic zone is coarse-grained as a Gaussian sink in Q space, as written in eq 3.4. Its relative position in the reaction funnel, its width in Q space, and its reaction time scale compared to the time scale of the Q coordinate relaxation all together determine the delicate coupling between the conformational dynamics of Q and the catalysis reaction at the sink. The three subsections introduced in section 6 illustrate such a coupling.

9. Conclusion

Let us summarize the main results of this paper. We have developed a 2D multisurface free-energy description to model enzyme-assisted biochemical reactions in solution, incorporating several important well-known features of catalysis. In particular, the transition-state stabilization mechanism of Pauling has been included in the formalism. The reaction free-energy surface consists of four distinct surfaces to account for the four distinct physical states involved in the entire catalytic process. In this description, the coordinate Q denotes the set of slow enzyme conformational modes that directly participate in the catalytic reaction. After the real-space diffusion of the substrate to the proximity of the enzyme, the next step is a thermally activated motion of the Q coordinate to accommodate the substrate, accomplished through enzyme conformational fluctuation. The enzyme−substrate binding transforms the reaction system to a new surface where catalysis takes place after the activation-energy-lowering conformational relaxation is completed. The last step provides a free-energy-based description of the concept of induced fit of Koshland. Catalysis leads to another surface transition: that of the enzyme−product complex, EP. In the last stage, product release leads to crossing to the last surface E···P. Then the cycle repeats itself.

We have used the free-energy surfaces to obtain a general theoretical framework to address the role of multi-time-scale protein conformational dynamics in the overall enzyme catalysis. The theoretical scheme employed invokes the Smoluchowski equation with a time-dependent diffusion constant, which is obtained from the experimental conformation fluctuation time correlation function, $\langle Q(0)Q(t)\rangle$. Once the Green function for propagation on the reaction surface is determined, we model the reactions on the free energy surfaces by reaction funnels with certain sink terms, in a spirit similar to the ones employed for barrierless isomerization reactions,[53] CO binding to heme protein,[54] and solvent effects on electron-transfer reactions.[55] We have obtained detailed numerical solution for several cases, as presented in Figures 10−13.

We have shown that the well-known MM expression of the rate remains valid, even under dispersive kinetics of enzyme fluctuations. We have also demonstrated that the time dependence of the catalysis of lipase B can be explained by the present theory with reasonable values of the parameters involved. The latter comparison (shown in Figure 12) is satisfying because it demonstrates both the robustness and the applicability of the theoretical scheme.

The theoretical analyses presented in sections 6 and 7 demonstrate that the competition between enzyme conformation fluctuation and catalysis rate may often determine the overall reaction dynamics. The results presented there show how the overall rate is dependent on the conformational dynamics whose time scales are comparable to or slower than that of the catalysis sink. That is, if the sink is efficient, then enzyme dynamics can become rate-determining. This is the limit that appears to have been reported in several recent NMR experiments where the rate of catalytic conversion is close to the rate of conformational fluctuation.[8−10] In the opposite limit of slow conversion rate at the sink, only the faster components of enzyme dynamics can be coupled to the reaction.

Thus, within this theoretical framework, two separately observable dynamical events—the single-molecule measurements on enzymatic reaction dynamics and the single-molecule experiments on protein conformational dynamics—have been semiquantitatively linked together under the general concept of "fluctuating enzymes".[3,56−63] The numerical calculations are shown to be in good semiquantitative agreement with observed results.

In the limit of low activation barrier along the X coordinate in the ES state, the optimal reaction trajectory will involve motions along both the X and Q coordinates. As a result, the trajectory is slanted along both the X and Q coordinates. This optimal reaction trajectory as well as the rate can be obtained by using the transition path sampling technique developed recently.[64]

It seems interesting to relate the current topic with the protein-folding problem. In order for the enzyme to perform its catalytic action, it might need to execute a rather large conformational fluctuation from its native state. However, it is well-known that too large a departure from the native state reduces the catalytic activity of the enzyme substantially. Actually, the extent of unfolding is often measured experimentally in terms of the reduction in the enzymatic activity of the protein. It is thus a rather complex issue, and we need to study specific instances to understand the extent and nature of enzyme conformational fluctuation around its native state. The natural fluctuations involved in the late stage of folding can be the same ones responsible for the slow time scales observed in enzyme dynamics. It is perhaps not a mere coincidence that the time scale of protein folding also lies in the window of sub-milliseconds to several hundred seconds for most proteins. This reminds one of the elegant approach of Zwanzig to model folding as a diffusion on a rugged harmonic surface[38] and gives further credence to our treatment of enzyme dynamics in terms of harmonic surfaces. It is certainly worthwhile to explore the relationship between the time scales of protein unfolding, the slow protein conformational dynamics observed in single molecule experiments, and the time scales of catalysis.

In a future study,[52] we shall show that the present theoretical scheme can be extended to understand the nature of the nonequilibrium steady state[65] of a functioning enzyme and also both the positive and negative cooperativity of substrate concentration dependence.

Acknowledgment. For this work, we are grateful to helpful discussions with Prof. Attila Szabo, Prof. Hong Qian, Mr. Liang Jiang, Dr. Jianhua Xing, Dr. Brian English, and Prof. M. Tachiya. X.S.X. acknowledges supports from DOE, and an NIH Director's Pioneer Award. B.B. thanks the department of Chemistry and Chemical Biology, Harvard University, for kind hospitality and Xie group members for discussions and interactions.

References and Notes

(1) Wolfenden, R.; Snider, M. J. *Acc. Chem. Res.* **2001**, *34*, 938.
(2) Michaelis, L.; Menten, M. L. *Biochem. Z.* **1913**, *49*, 333.
(3) Welch, G. R. ed. *The Fluctuating Enzyme*; Wiley: New York, 1986.
(4) Hammes, G. G. *Biochemistry* **2002**, *41*, 8221.
(5) See the thematic issue on the principle of enzymatic catalysis of *Chem. Rev.* **2006**, *106*, 8.
(6) Hammes-Schiffer, S.; Benkovic, S. J. *Annu. Rev. Biochem.* **2006**, *75*, 519.
(7) Garcia-Viloca, M.; Gao, J.; Karplus, M.; Truhlar, D. G. *Science* **2004**, *303*, 186.
(8) Wolf-Watz, M.; Thai, V.; Henzler-Wildman, K.; Hadjipavlou, G.; Eisenmesser, E. Z.; Kern, D. *Nat. Struct. Mol. Biol.* **2004**, *11*, 945.
(9) Kern, D.; Eisenmesser, E. Z.; Wolf-Watz, M. *Methods Enzymol.* **2005**, *394*, 507.
(10) Eisenmesser, E. Z.; Millet, O.; Labeikovsky, W.; Korzhnev, D. M.; Wolf-Watz, M.; Bosco, D. A.; Skalicky, J. J.; Kay, L. E.; Kern, D. *Nature* **2005**, *438*, 117.
(11) Yang, H.; Luo, G.; Karnchanaphanurach, P.; Louie, T.-M.; Rech, I.; Cova, S.; Xun, L.; Xie, X. S. *Science* **2003**, *302*, 262.
(12) Kou, S. C.; Xie, X. S. *Phys. Rev. Lett.* **2004**, *93*, 180603−180607.
(13) Min, W.; Luo, G.; Cherayil, B. J.; Kou, S. C.; Xie, X. S. *Phys. Rev. Lett.* **2005**, *94*, 198302(1)−198302(4).
(14) Kramers, H. A. *Physica* **1940**, *7*, 284.
(15) Zwanzig, R. *Nonequilibrium Statistical Mechanics*; Oxford University Press: New York, 2001.
(16) Grote, R. F.; Hynes, J. T. *J. Chem. Phys.* **1980**, *73*, 2715; Hynes, J. T. *Annu. Rev. Phys. Chem.* **1985**, *36*, 573.
(17) Min, W.; Xie, X. S. *Phys. Rev. E* **2006**, *73*, 010902.
(18) Chaudhury, S.; Cherayil, B. J. *J. Chem. Phys.* **2006**, *125*, 114106.
(19) Florián, J.; Goodman, M. F.; Warshel, A. *Proc. Natl. Acad. Sci. U.S.A.* **2005**, *102*, 6819.
(20) Pauling, L. *Chem. Eng. News* **1946**, *24*, 1375.
(21) Schowen, R. L. In *Transition States of Biochemical Processes*; Gandour, R. D., Schowen, R. L., Eds.; Plenum: New York, 1978; p 77.
(22) Shokat, K. M.; Schultz, P. G. *Annu. Rev. Immunol.* **1990**, *8*, 335.
(23) Koshland, D. E. *Proc. Natl. Acad. Sci. U.S.A.* **1958**, *44*, 98.
(24) Fersht, A. *Structure and Mechanism in Protein Science: A Guide to Enzyme Catalysis and Protein Folding*; Freeman: New York, 1999.
(25) Bustamante, C.; Chemla, Y. R.; Forde, N. R.; Izhaky, D. *Annu. Rev. Biochem.* **2004**, *73*, 705.
(26) McCammon, J. A.; Northrup, S. H. *Nature* **1981**, *293*, 316.
(27) Szabo, A.; Shoup, D.; Northrup, S. H.; McCammon, J. A. *J. Chem. Phys.* **1982**, *77*, 4484.
(28) Austin, R. H.; Beeson, K. W.; Eisentein, L.; Frauenfielder, H.; Gunsalus, I. C. *Biochemistry* **1975**, *14*, 5355.
(29) Lim, M.; Jackson, T. A.; Anfinrud, P. A. *Proc. Natl. Acad. Sci. U.S.A.* **1993**, *90*, 5801.
(30) Hagen, S. T.; Eaton, W. A. *J. Chem. Phys.* **1996**, *104*, 3395.
(31) Suckau, D.; Shi, Y.; Beu, S. C.; Senko, M. W.; Quinn, J. P.; Wampler, F. M., III; McLafferty, F. W. *Proc. Natl. Acad. Sci. U.S.A.* **1993**, *90*, 790.
(32) Lu, H. P.; Xun, L.; Xie, X. S. *Science* **1998**, *282*, 1877.
(33) van Oijen, A. M.; Blainey, P. C.; Crampton, D. J.; Richardson, C. C.; Ellenberger, T.; Xie, X. S. *Science* **2003**, *301*, 1235.
(34) Velonia, K.; Flomenbom, O.; Loos, D.; Masuo, S.; Cotlet, M.; Engelborghs, Y.; Hofkens, J.; Rowan, A. E.; Klafter, J.; Nolte, R. J. M.; de Schryver, F. C. *Angew. Chem., Int. Ed.* **2005**, *44*, 560.
(35) Flomenbom, O.; Velonia, K.; Loos, D.; Masuo, S.; Cotlet, M.; Engelborghs, Y.; Hofkens, J.; Rowan, A. E.; Nolte, R. J. M.; van der Auweraer, M.; de Schryver, F. C.; Klafter, J. *Proc. Natl. Acad. Sci. U.S.A.* **2005**, *102*, 2368.
(36) English, B. P.; Min, W.; van Oijen, A. M.; Lee, K. T.; Luo, G.; Sun, H.; Cherayil, B. J.; Kou, S. C.; Xie, X. S. *Nat. Chem. Biol.* **2006**, *2*, 87.
(37) Hatzakis, N. S.; Engelkamp, H.; Velonia, K.; Hofkens, J.; Christianen, P. C. M.; Svendsen, A.; Patkar, S. A.; Vind, J.; Maan, J. C.; Rowan, A. E.; Nolte, R. J. M. *Chem. Commun.* **2006**, *19*, 2012.
(38) Zwanzig, R. *Proc. Natl. Acad. Sci. U.S.A.* **1988**, *85*, 2029.
(39) Onuchic, J. N.; Luthey-Schulten, Z.; Wolynes, P. G. *Annu. Rev. Phys. Chem.* **1997**, *48*, 545.
(40) Leopold, P. E.; Montal, M.; Onuchic, J. N. *Proc. Natl. Acad. Sci. U.S.A.* **1992**, *89*, 8721.
(41) Onuchic, J. N.; Wolynes, P. G. *Curr. Opin. Struct. Biol.* **2004**, *14*, 70.
(42) Roca, M.; Moliner, V.; Tuñón, I.; Hynes, J. T. *J. Am. Chem. Soc.* **2006**, *128*, 6186.
(43) Skinner, J. L.; Wolynes, P. G. *J. Chem. Phys.* **1978**, *69*, 2143.
(44) Neria, E.; Karplus, M. *Chem. Phys. Lett.* **1997**, *267*, 23.
(45) Okuyama, S.; Oxtoby, D. W. *J. Chem. Phys.* **1986**, *84*, 5824.
(46) Hynes, J. T. *J. Phys. Chem.* **1986**, *90*, 3701.
(47) Min, W.; Gopich, I. V.; English, B. P.; Kou, S. C.; Xie, X. S.; Szabo, A. *J. Phys. Chem. B* **2006**, *110*, 20093.
(48) Wang, H.; Oster, G. *Nature* **1998**, *396*, 279.
(49) Luo, G.; Wang, M.; Konigsberg, W. H.; Xie, X. S. *Proc. Natl. Acad. Sci. U.S.A.* **2007**, *104*, 12610.
(50) Akesson, E.; Walker, G. C.; Barbara, P. F. *J. Chem. Phys.* **1991**, *95*, 4188.
(51) Zusman, L. D. *Chem. Phys.* **1980**, *49*, 295.
(52) Min, W; Xie, X. S.; Bagchi, B. To be submitted for publication.
(53) Bagchi, B.; Fleming, G. R.; Oxtoby, D. W. *J. Chem. Phys.* **1983**, *78*, 7375.
(54) Agmon, N.; Hopfield, J. J. *J. Chem. Phys.* **1983**, *78*, 6947.
(55) Sumi, H.; Marcus, R. A. *J. Chem. Phys.* **1986**, *84*, 4894.
(56) Min, W.; English, B. P.; Luo, G.; Cherayil, B. J.; Kou, S. C.; Xie, X. S. *Acc. Chem. Res.* **2005**, *38*, 923.
(57) Yang, S.; Cao, J. *J. Chem. Phys.* **2002**, *117*, 10996.
(58) Agmon, N. *J. Phys. Chem. B* **2000**, *104*, 7830.
(59) (a) Gopich, I. V.; Szabo, A. *J. Chem. Phys.* **2006**, *124*, 154712. (b) Kou, S. C.; Cherayil, B. J.; Min, W.; English, B. P.; Xie, X. S. *J. Phys. Chem. B* **2005**, *109*, 19068. (c) Xing, J. *Phys. Rev. Lett.* **2007**, *99*, 168103.
(60) Lerch, H. P.; Rigler, R.; Mikhailov, A. S. *Proc. Natl. Acad. Sci. U.S.A.* **2005**, *102*, 10807.
(61) Karplus, M. *J. Phys. Chem. B* **2000**, *104*, 11.
(62) Engelkamp, H.; Hatzakis, N. S.; Hofkens, J.; De Schryver, F. C.; Nolte, R. J. M.; Rowan, A. E. *Chem. Commun.* **2006**, *37*, 935.
(63) Luo, G.; Andricioaei, I.; Xie, X. S.; Karplus, M. *J. Phys. Chem. B* **2006**, *110*, 9363.
(64) Bolhuis, P. G.; Chandler, D.; Dellago, C.; Geissler, P. *Annu. Rev. Phys. Chem.* **2002**, *53*, 291.
(65) Qian, H. *J. Phys. Chem. B* **2006**, *110*, 15063.